Advanced non-quasi-static(NQS) compact model for characterization of non-resonant plasmonic terahertz detector

Sang Hyo Ahn, Min Woo Ryu, Esan Jang, Hyeong Ju Jeon and Kyung Rok Kim*
School of Electronic and Computer Engineering
Ulsan National Institute of Science and Technology (UNIST)
Ulsan 44919, Republic of Korea
krkim@unist.ac.kr*

***Abstract*— We propose advanced non-quasi-static (NQS) compact model of field-effect transistor (FET) for the characterization of a non-resonant plasma-mode terahertz (THz) detector in THz frequency regime by verifying the gate resistance effects on the transient delay and non-resonant plasmonic mechanism with characteristic length, which is a propagation distance of 2-dimensional electron gas (l_{2DEG}), in the channel. Under the super-imposed small-signal ac voltage with 0.2 THz frequency in HSPICE simulation, the plasmonic THz power detection simulation capability of the proposed NQS model has been verified by demonstrating the well-matched results of dc output voltage (Δu) with calibrated TCAD and experimentally measured data. These results can provide the reliable circuit simulation platform for real-time multi-pixel THz imaging operation.**

Keywords—non-quasi-static; compact model; non-resonant; plasmonic; tehaertz; detector; real-time THz imaging

I. INTRODUCTION

Recently, the research on terahertz (THz) detection incorporating the plasmonic behavior has been performed in the various fields including real-time imaging application, biomedical, and even satellite communication [1]-[5]. The potential come from its unique properties, which include permeability of the microwaves and feature of straight of light. For detecting the THz wave, the field-effect transistors (FETs) have been intensively considered for THz detector in non-resonant plasma-mode [6]-[7], and many circuit integrated THz detectors also have been reported [8]-[11]. It becomes essential to establish the non-quasi-static (NQS) model of FET-based plasmonic detector in the THz regime for the practical design of the real-time multi-pixel configuration. In terms of the accurate analysis of fast switching [12]-[13] and high-frequency operation [14]-[15], however, most of the NQS FET models have the complexity of the formulation and fail to describe the plasmonic detecting operation [16].

In this work, we developed the equivalent circuit compact model of a silicon (Si) MOSFET-based plasmonic THz detector. The advanced NQS compact model for a plasmonic MOSFET is developed by verifying both the gate resistance

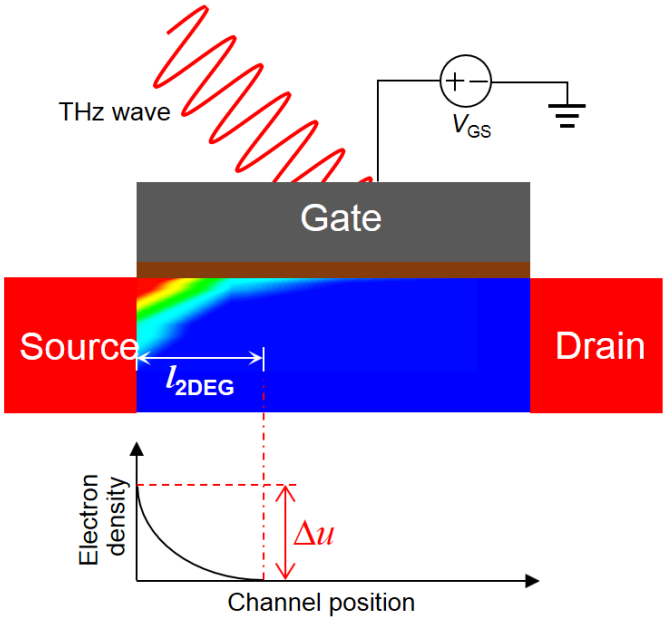

Fig. 1. Electron density of Cross-sectional schematic in channel at non-resonant detection mode, low frequency and low mobility detector ($\omega\tau$ <<1). electron density increase near the source. And it attenuate as far from the source.

effect on the transient delay and terahertz detection delay as a function of gate voltage. As a result, our model well matched with experimentally measured data and the numerical 3-D technology computer aided design (TCAD) simulation using the proposed NQS compact model in H-simulation program with integrated circuit emphasis (HSPICE) BSIMv3 circuit simulation.

II. NQS COMPACT MODEL FOR THZ DETECTOR

For modeling of non-resonant terahertz detection mechanism, it is important to describe plasma wave motion. Based on plasma wave theory, plasma wave decay until the propagation length of plasma wave defined as l_{2DEG}, given by [17],

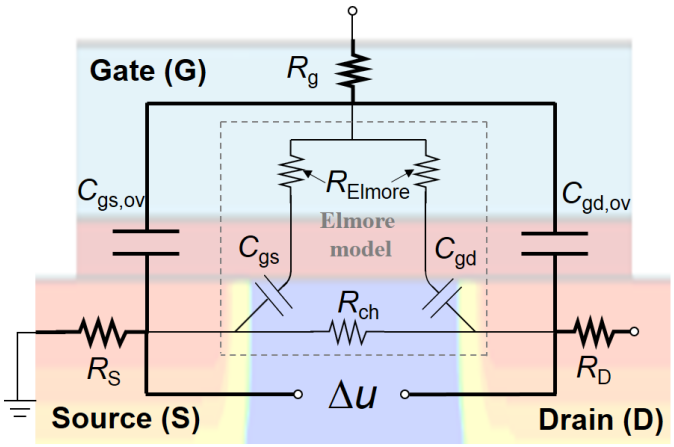

Fig. 2. Equivalent circuit configuration of the advanced NQS model from an Elmore model (dashed box) for plasmonic MOSFET operation with a THz detection output(Δu).

$$l_{2DEG} = \sqrt{\frac{\mu n}{\omega (dn/dU)|_{U=U_{ov}}}} \quad (1)$$

where

$$n(U) = \frac{C\eta k_B T}{e^2} \ln\left[1+\exp\left(\frac{eU}{\eta k_B T}\right)\right] \quad (2)$$

here, n is the electron concentration of channel $\omega$is the frequency of the external radiation, μ is mobility, C is the gate-to-channel capacitance per unit area, k_B is Boltzmann constant, T is temperature, e is the electron charge, η is the subthreshold ideality factor, and U is the gate to channel voltage swing, given by $U = U_{ov}$-U_{ch}, where $U_{ov} = U_g - U_t$ is the voltage swing, U_g and U_{ch} are the gate and threshold voltages, respectively, and U_{ch} is the channel voltage. As shown in Fig. 1, plasma wave potential generated by electron density is overdamped from source to drain in the channel. Even if when $L_g > l_{2DEG}$, Δu is saturated, when $L_g < l_{2DEG}$, Δu is increased as a function of gate length.

Figure 2 shows the equivalent circuit configuration of our advanced NQS model for plasmonic MOSFET operation. The distinguished features of our proposed model in contrast with the Elmore model (dashed line box), which is widely used as NQS model, include the additional resistance of the gate (R_g), source (R_S), and drain (R_D) as well as the additional capacitance of the gate-to-drain ($C_{gd,ov}$) and source overlap capacitance ($C_{gs,ov}$) for satisfying asymmetric boundary condition between source and drain [18].

To verify the model on the physical R_g effect in transit mode, large-signal DC transient gate delay characteristics according to Al (metal), NiSi (silicide), and poly-Si gate materials are compared with the numerical TCAD simulation

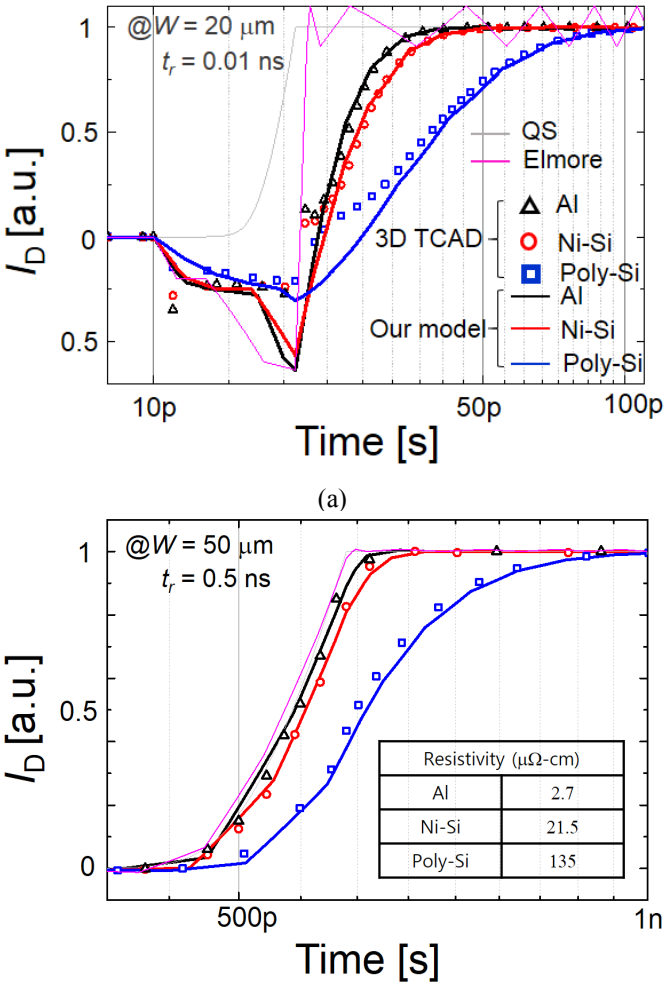

Fig. 3. Transient gate delay simulation results for Al, NiSi and poly-Si gate materials from the proposed NQS model compared with 3D TCAD. (a) W = 20 μm, t_r = 10ps (b) W = 50 μm, t_r = 500ps.

based on common material-dependent resistivity (ρ), ρ_{Al}= 2.7 μΩ-cm, ρ_{NiSi}= 21.5 μΩ-cm, and $\rho_{poly\text{-}Si}$= 135 μΩ-cm, as shown in Fig. 3. Under the gate voltage (V_G) with increasing time of both 0.01 and 0.5 ns, the transient simulation results of the drain current (I_D) from our model are well-matched with the numerical 3-D TCAD simulation results by describing the gate width (W= 20, 50 μm) effects on the I_D delay, while the Elmore model shows similar results with the quasi-static (QS) model that cannot describe the R_g effect on the transient delay characteristics.

In non-resonant mode plasmonic THz detection mechanism, characteristic length, which is a propagation distance of 2-D electron gas (l_{2DEG}), is occurred by asymmetric electron density oscillation in the channel when THz wave is radiated [18]. If L_g is shorter than l_{2DEG} (= $s(\tau/\omega)^{0.5}$, where s is plasma wave velocity, τ is momentum relaxation time [19]), DC offset voltage (Δu) is not observed owing to symmetry condition in the channel as shown in Fig. 4 This l_{2DEG} is depended on incoming THz wave frequency as shown

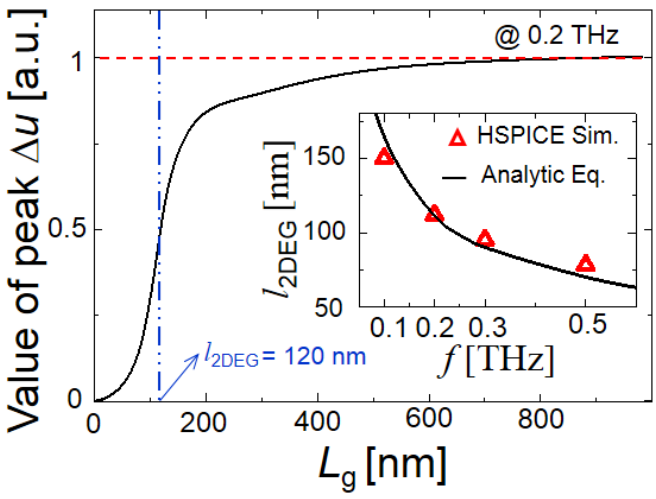

Fig. 4. The value of peak Δu as a function of gate length. DC offset voltage (Δu) increase with increasing gate length at V_{ov} = 0V. Inset shows l_{2DEG} as a function of incoming THz wave frequency compared with analytic equation.

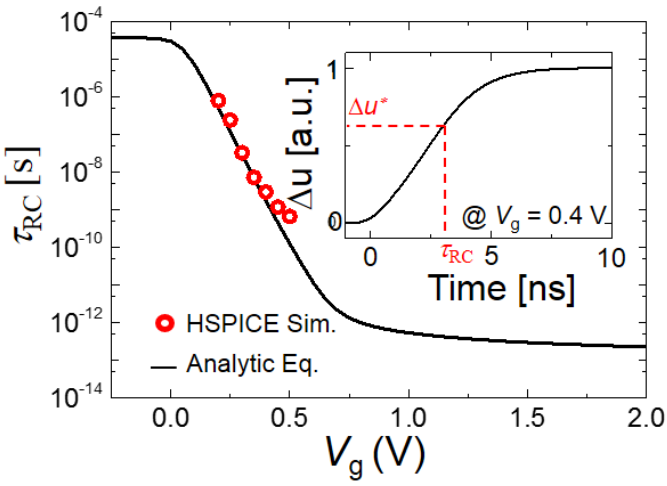

Fig. 5. This figure shows RC time constant calculated from THz detection delay simulation as a function of gate voltage. Inset shows intrinsic THz detection delay simulation is defined from $\Delta u(t) = \Delta u(\infty)\{1\text{-}\exp(-t/\tau_{RC})\}$ in subthreshold regime.

in the inset of Fig. 4. l_{2DEG} is depended on incoming THz wave frequency as shown in the inset of Fig. 4.

The plasma wave propagation length determines terahertz detection delay, given by [19]

$$\tau_{RC} = R(l_{2DEG})C(l_{2DEG}) = l_{2DEG}{}^2 \frac{\rho}{t_{2DEG}} C \qquad (3)$$

Here ρ is resistivity of channel and t_{2DEG} is thickness of 2DEG. Based on the l_{2DEG}, the intrinsic THz detection delay can be estimated by an analytic equation as shown in Fig. 5. This intrinsic THz detection delay time is defined from $\Delta u(t) = \Delta u(\infty)\{1\text{-}\exp(-t/\tau_{RC})\}$ in subthreshold regime (inset). Δu^* is

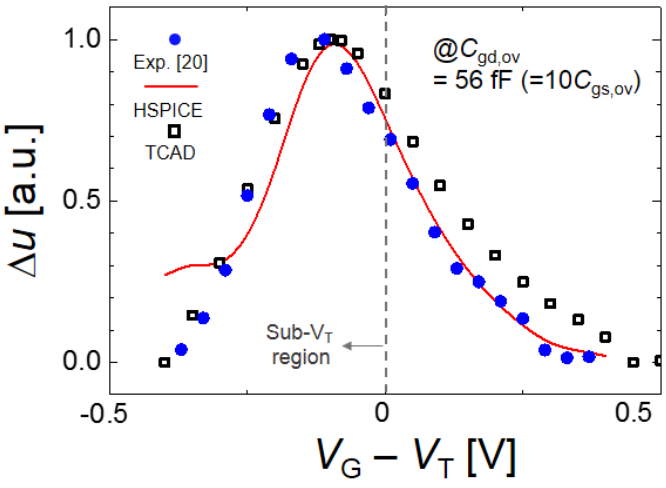

Fig. 6. The well-matched HSPICE simulation results of Δu as a function of the gate overdrive voltage (V_G - V_T) at $C_{gd,ov}$(=10$C_{gs,ov}$) with TCAD simulation and Experiment.

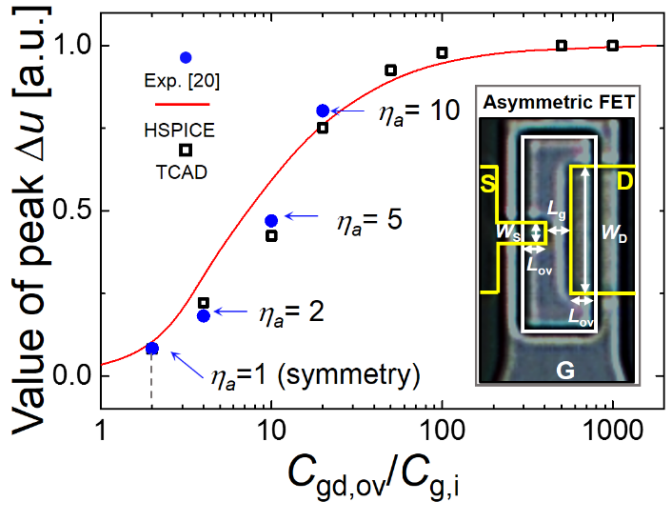

Fig. 7. HSPICE simulation results of value of peak Δu as a function of $C_{gd,ov}/C_{g,i}$ with experiment and mixed-mode TCAD.

defined by $\Delta u(\tau_{RC}) = \Delta u(\infty)\{1\text{-}1/e)\}$. From the (3), l_{2DEG} can be expressed by $(t_{2DEG}\tau_{RC}/\rho C)^{0.5}$. When τ_{RC} = 2.98 ns, C = 863 nF/cm^2, t_{2DEG} = 3 nm and ρ = 5.68 Ω-cm, propagation length is 135 nm. It is similar with propagation length getting from Fig. 4. From the results, our NQS model can fully describe non-resonant plasmonic channel in THz regime.

III. Result and Discussion

As shown in Fig. 6, under the super-imposed small-signal AC voltage on the gate ($v_{ac} = v_a \sin 2\pi ft$, v_a= 20 mV, f=0.2 THz), the plasmonic THz power detection simulation capability of the proposed NQS model has been verified by demonstrating the well-matched results of the Δu with calibrated TCAD and experimentally measured data. The key model parameters of the asymmetric $C_{gd,ov}$= 56 fF(= 10$C_{gs,ov}$) by the gate oxide thickness of T_{ox}= 50 nm under W_D= 20 μm(= 10W_S) with the

same L_{ov}= 4 μm and R_g= 72.15 Ω for the Al gate are used based on the HSPICE BSIMv3 model.

Furthermore, the asymmetric $C_{gd,ov}$ effect on the peak Δu has also been verified with good agreement for the normalized peak Δu as a function of the ratio of $C_{gd,ov}$ and the intrinsic gate-to-channel capacitance ($C_{g,i}$) between the model and mixed-mode TCAD with external gate-to-drain capacitance ($C_{gd,ext}$)= $C_{gd,ov}$, as shown in Fig. 7. Inset of Fig.7 shows THz plasmonic Si-FET, which has the asymmetric overlap width of the source (W_S= 2 μm) and drain (W_D= 20 μm) under the same channel (L_g= 2 μm) and overlap lengths (L_{ov}= 4 μm) [20]. Based on the Si-FET, he $C_{gd,ov}/C_{g,i} > 1$ is the key condition to enhance the performance (peak Δu) of the plasmonic THz detector [6]. The values of peak Du from the experimental MOSFET with various asymmetry ratio (η_a= $C_{gd,ov}/C_{gs,ov}$= $C_{gd,ov}/2C_{g,i}$) from η_a= 1 (symmetry) to 10 have also been plotted exactly on the HSPICE simulation results from the proposed NQS compact model.

IV. Conclusion

In conclusion, we have verified characterization of non-resonant mode plasmonic THz detector based on FETs by using our proposed advanced NQS compact model. These results can provide the reliable circuit simulation platform for real-time multi-pixel THz imaging operation.

Acknowledgment

This work was supported by the Pioneer Research Center Program (Grant No. 2012-0009600) and by Mid-career Research Program (Grant No. 2015R1A2A2A04005910) through the National Research Foundation of Korea funded by the Ministry of Science, ICT & Future Planning.

References

[1] P. H. siegel, "Terahertz technology," *IEEE Trans. Microw. Theory Techn.*, vol. 50, no. 3, pp. 910-928, Mar. 2002.

[2] P. H. siegel, "Terahertz Technology in Biology and Medicine," *IEEE Trans. Microw. Theory Techn.* vol. 52, no. 10, pp. 2438-2447, Oct. 2004.

[3] M. C. Kemp, P. F. Taday, B. E. Cole, J. A. Cluff, A. J. Fitzgerald, W R Tribe "Security application of terhaertz technology," Proceedings of SPIE, vol. 5070, pp. 44-52, 2003.

[4] M. Tonouchi, "Cutting-edge terahertz tchnology," *Nature photonics,* vol. 1, pp. 97-105, 2007.

[5] E. Pickwell and V. P. Wallace, "Biomedical applications of terhaertz technology,"*J. Phys. D, Appl. Phys*., vol. 39, R301-R310, 2006.

[6] M. Dyakonov and M. Shur, "Detection, Mixing, and Frequency Multiplication of Terahertz Radiation by Two-Dimensional Electronic Fluid," *IEEE T- ED*, vol. 43, no. 3, pp. 380-387, March. 1996

[7] A. Gutin, V. Kachorovskii, A. Muraviev, and M. shur, "Plasmonic terahertz detector response at high intensities," *J. Appl. Phys.* vol. 112, 014508, 2012.

[8] S. Boppel, A. Lisauskas, A. Max, V. Krozer, and H.G. Roskos, "CMOS detector arrays in a virtual 10-kilopixel camera for coherent terahertz real-time imaging," *opt. letters*., vol. 37, no. 4, pp.536-538 ,Feb. 2012.

[9] R. Al. Hadi, H. Sherry, J. Grzyb, Y. Zhao, W. Förster, H. M. Keller, A. Cathelin, A. Kaiser, and U. R. Pfeiffer, "A 1 k-Pixel Video Camera for 0.7-1.1 Terahertz Imaging Applications in 65-nm CMOS," *IEEE J. Solid-State Circuits*, vol. 42, no. 12, pp. 2999-3012, Dec. 2012.

[10] J.-R. Yang, W.-J. Lee, and S.-T. Han, "Signal-conditioning Block of a 1x200 CMOS Detector Array for a Terahertz Real-Time Imaging System," *Sensors*, vol.16, no. 3, pp.319-329, Mar, 2016.

[11] M. W. Ryu, S.H. Ahn, J.-R. Yang, W.-J. Lee, S.-T. Han, K.R.Kim, "Plasmonic 1x200 Array Scanner based on 65-nm CMOS Asymmetric FETs for Real-Time Terahertz," in Proc. 74th Device Research Conference, Jun. 2016.

[12] M. Chan, K.Y. Hui, C. Hu, and P.K. Ko, "A Robust and Physical BSIM3 Non-Quasi-Static Transient and AC Small-Signal model for Circuit Simulation," *IEEE Transactions on Electron Devices*, vol. 45, no 4, pp.834-841, Apr, 1998.

[13] H. Wang, X. Li, W. Wu, G. Gildenblat, R.v. Langevelde, G.D.J. Smit, A.J. Scholten, and K.B.M. Klaassen, "A Unified Nonquasi – Static MOSFET Model for Large-Signal and Small-Signal Simulations" *IEEE Transactions on Electron Devices*, vol, 53, no. 9, pp.2035-2043, Sep 2006.

[14] E. Ojefors, U.R. Pfeilffer, A. Lisauskas, and H.G. Roskos, "A 0.65 THz focal-plane array in a quarter-micron CMOS process technology," *IEEE J. Solid-State Circuits*, vol. 44, no. 7, pp. 1968-1976, Jul., 2009.

[15] S. Boppel, A. Lisauskas, M. Mundt, D. Seliuta, L. Minkevicius, I. Kasalynas, G. Valusis, M. Mittendorff, S. Winnerl, V. Krozer, and H.G. Roskos, "CMOS Integrated Antenna-Coupled Field-Effect Transistors for the Detection of Radiation From 0.2 to 4.3THz," *IEEE Transactions on Micorwave Theory and Techniques*, vol. 60, no.12, pp. 3834-3843, Dec,2012

[16] A. Gutin, T. Ytterdal, V. Kachorovskii, A. Muraviev, and M. Shur, "THz SPICE for Modeling Detectors and Nonquadratic Response at Large Input Signal," *IEEE Sensors Journal*, vol, 13, no. 1, pp. 55-62, Jan 2013.

[17] A. Gutin, V. Kachorovskii, A. Muraviev, and M.Shur, "Plasmonic terahertz detector response at high intensities," *Journal of Applied Physics*, vol. 112, pp. 014508, 2012.

[18] M. W. Ryu, J.S. Lee, K.S. Kim, K. Park, J.R. Yang, S.-T. Han, and K.R. Kim, "High Perfomance Plasmonic THZ detector on Asymmetric FET with Vertically Integrated Antenna in CMOS Technologe." *IEEE Transactions on Electron Devices*, vol. 63, no 4, pp.1742-1748, Apr 2016.

[19] W. Knap, M. Dyakonov, D. Coquillat, F. Teppe, N Dyakonova, J Lusakowski, K. Karpierz, M. Sakowicz, G. Valusis, D. Seliuta, I. Kasalynas, A. EL Fatimy, Y. M. Meziani, and T. Otsuji, "Field Effect Transistors for Terahertz Detection: Physics and First Imaging Applications," *J Infrared Milli Terahertz Waves*, vol. 30, 1319, 2009.

[20] M. W. Ryu J. S. Lee, K. Park, W.-K. Park, S.-T. Han, and K. R. Kim, "Photoresponse enhancement of plasmonic terahertz wave detector based on asymmetric silicon MOSFETs with antenna integration," *Jpn. J. Appl. Phys*., vol. 53, no. 4S, p. 04EJ05, Apr. 2014.